Nuclear magnetic shielding of nitrogen in ammonia

Cynthia J. Jameson and Angel C. de Dios
Department of Chemistry, M/C-111, University of Illinois at Chicago, Chicago, Illinois 60680

A. Keith Jameson
Department of Chemistry, Loyola University, Chicago Illinois 60626

(Received 31 December 1990; accepted 2 April 1991)

The nitrogen shielding surface in ammonia is calculated using the localized orbital-local origin (LORG) method of Hansen and Bouman, in terms of the symmetry coordinates for the molecule. With respect to the inversion coordinate, the *N* shielding surface has a shape similar to the potential surface. Rovibrational averaging of the *N* shielding in NH_3 and ND_3 molecules is carried out using numerical wave functions which are solutions to the inversion potential which best fits the spectra of all isotopomers. The other coordinates are vibrationally averaged in the usual way, assuming small amplitude motions. The calculated temperature dependence of the *N* shielding due to inversion is in the opposite sense to that observed for a large number of molecules, and is nearly canceling the contributions from all the other coordinates. The temperature dependence of the nitrogen shielding in ammonia has been measured in the range 300–400 K in samples with densities in a hundredfold range (0.37–33 amagat). When the temperature-dependent intermolecular effects are separated out, the remaining temperature dependence is small and is consistent with the calculations. The inversion contribution to the deuterium-induced isotope shift is of opposite sign to the contributions from all other coordinates. The agreement with the experimental isotope shift in the liquid phase is satisfactory.

INTRODUCTION

Molecular electronic properties which are measured in the laboratory are averages over the nuclear configurations which the molecule traverses as it undergoes rotation and vibration. Within the Born–Oppenheimer approximation, there is a unique value of the electronic property for each arrangement of nuclei and the collection of all such values as a function of nuclear configuration space constitutes the molecular electronic property surface. On the other hand, the probability of finding the molecule in a particular nuclear arrangement is governed by the potential energy surface. Every measured value of a molecular electronic property is an average over such probabilities if measured for a specific rovibrational state, or a further average of the values for many rovibrational states by population if measured as a thermal average. The thermal average value should exhibit both an isotope effect and a temperature dependence, each one being a measure of the unique way in which the probabilities of various nuclear configurations are dependent on nuclear masses and the distribution over different energy levels. Conversely, the observed isotope effects and temperature dependence provide some information about the shape of the property surface in that part of the nuclear configuration space which constitutes the deep pocket in the intramolecular potential surface, i.e., in the immediate vicinity of the equilibrium molecular geometry. On the experimental side, nuclear magnetic resonance spectroscopy in the gas phase allows precise measurements of some magnetic properties such as nuclear magnetic shielding and spin–spin coupling, as a function of temperature, and in favorable cases, the isotope effects can also be observed. On the theoretical side, computations of intramolecular potential energy surfaces and also molecular electronic property surfaces are currently in progress in many laboratories, with the limitations of both being scrutinized via comparisons with experiment.

Ammonia is of particular interest because of what appeared to be an exceptional temperature dependence exhibited by the nitrogen (but not the proton) resonance frequency,[1] this being the only such unusual case other than ^{31}P in PH_3.[2] We have since remeasured the ^{31}P temperature dependence in PH_3 in samples of much lower density and find the temperature dependence of the intermolecular effects on the shielding had not been sufficiently precisely determined in the earlier work, leaving the "observed" intrinsic temperature dependence partly contaminated with the temperature dependence of the intermolecular effects.[3] This leaves N in NH_3 as the only unusual case. The earlier measurements had been made at 9.1 MHz in a 2.1 tesla magnet.[1] The electromagnet drift characteristics required stabilization with the use of a lock substance outside the sample whose resonance frequency temperature dependence could only be obtained in an indirect way. Furthermore, given the limited sensitivity at 2.1 tesla, measurements were limited to samples of density higher than 12 amagat. Some contamination of the apparent zero-density temperature dependence by any small residual highly temperature-dependent intermolecular effects was of unknown magnitude. Earlier rovibrational averaging[4] for NH_3/ND_3 attempted to reconcile the apparent discrepancy between the exceptional observed temperature dependence of the shielding[1] and the deuterium-induced isotope shift[5] which was in the usual direction. However, without the shielding surface, these calculations could only provide limiting case scenarios for the dependence of the shielding on the N–H bond stretch and the H–N–H angle change. Moreover, the earlier discussions and

 0021-9606/91/141069-11$03.00

calculations assumed all vibrational amplitudes to be small and limited to one minimum, whereas in NH_3, the barrier to inversion is low enough that the molecule does not stay in one minimum. The inversion averaging of the shielding has to be done properly to allow for barrier penetration.

The objectives of this work were the following: to make more accurate measurements of the temperature dependence of the ^{15}N nuclear magnetic shielding in ammonia, so as to more precisely separately determine the intermolecular effects and the rovibrational averaging; both give rise to a temperature dependence of the nitrogen nuclear resonance frequency. Second, we wished to carry out *ab initio* calculations of the nitrogen shielding surface in ammonia. Third, we sought to do a proper averaging over the inversion coordinates using the full shielding surface and the numerical vibrational functions for inversion. In the comparison of theory with experiment, we expect to shed some light on the apparent discrepancy between the temperature dependence and the isotope shift data for this molecule and also to examine the differences between the carbon shielding surface in CH_4 and the nitrogen shielding surface in NH_3, if any, which may be attributed to the lone pair contributions to the shielding in the latter.

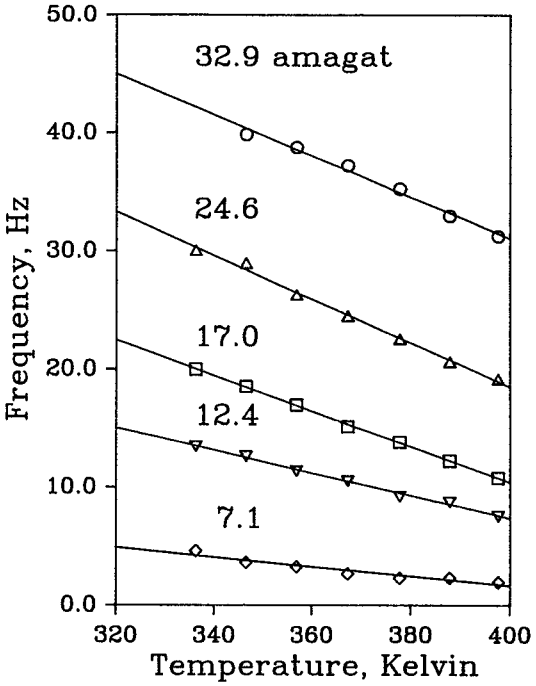

FIG. 1. ^{15}N resonance frequencies at 40.56 MHz in NH_3 in the gas phase.

EXPERIMENTAL

^{15}N spectra were obtained at 40.56 MHz in a Bruker AM-400 Fourier transform nuclear magnetic resonance (FT NMR) spectrometer in sealed 4 mm. (o. d.) tubes containing 99% ^{15}N-labeled NH_3 at relatively high densities (7–30 amagat). One amagat is the density of an ideal gas at standard temperature and pressure, i.e., 2.687×10^{19} molecules cm^{-3}. For the low density samples (0.3–1.5 amagat), sealed 9 mm (o. d.) tubes were used to compensate for the lower sensitivity at these low number densities. A typical spectrum had 1000–4000 transients and a resolution of, at least, 0.3 Hz/point. Temperatures were measured using a sealed sample of ethylene glycol. Temperature-dependent instrumental sources of resonance frequency changes such as field drift and changes in probe characteristics were monitored as follows: The stability of the external magnetic field at the sample for a period of 24 h upon changing temperature without altering any shim setting was ascertained to 0.01 ppm by monitoring the ^{13}C resonance in a sealed gas sample of methane. The ^{13}C shielding in methane is known to have a very small temperature dependence even at densities far from zero.[6] In any case, the theoretically predicted shift of ^{13}C in CH_4 for 300–400 K is only 0.016 ppm.[7] All measurements were done without the use of a lock solvent.

With the low density samples, gated $\{^1H\}$ decoupling was performed. At low densities, relaxation times become evidently shorter leading to much broader lines. For this reason, the peaks of the spectra were fitted to Lorentzians for more precise location of the center of the resonance in the low density samples. Phasing of the spectra being different for each temperature, the fitting was done for spectra obtained at various phase settings, the best one determined by examining the residuals.

Figure 1 shows the temperature dependence of the ^{15}N resonance frequency in the high density samples, from which density dependence the intermolecular effects on the shielding could be determined. Shown in Fig. 2, the second virial coefficient of the nitrogen shielding in

$$\sigma(T,\rho) = \sigma_0(T) + \sigma_1(T)\rho + \cdots \quad (1)$$

is found to be

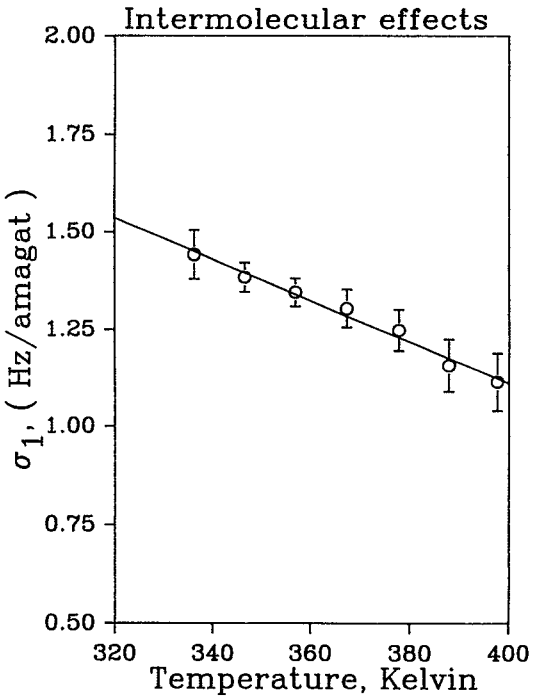

FIG. 2. The temperature dependence of the density coefficient of the nitrogen chemical shift.

$$\sigma_1(T) \text{ ppm amagat}^{-1} = -(0.0369 \pm 0.0009) + (1.32\times10^{-4})(T/K - 350) \quad (2)$$

corrected for bulk susceptibility. The value of σ_1 is obtained at each temperature from the linear dependence of the resonance frequency on the density of the sample. This may be compared with the old value[1] $\sigma_1(T) = 0.0408 \pm 0.002$ ppm amagat^{-1}, which when corrected for bulk susceptibility, equals 0.0393 ppm amagat^{-1}. Due to lack of precision, no temperature dependence had been reported.

When the value of $\sigma_1(T)\rho$ from Eq. (2) is subtracted from each resonance frequency in Fig. 1, the temperature dependence that remains is that of $\sigma_0(T)$. These points are shown in Fig. 3 together with the data points for the 0.37 amagat sample. The increase in linewidth with decreasing density leads to a larger scatter in the temperature dependence of this lowest density sample than can be obtained from the five high density samples after correction for $\sigma_1(T)\rho$. Nevertheless, the data appear to be consistent. The result is clearly a very small temperature dependence for the nitrogen shielding in the isolated NH_3 molecule.

AB INITIO CALCULATIONS OF THE SHIELDING SURFACE

The methods of calculation of nuclear magnetic shielding are reviewed regularly[8] and will not be discussed in detail here. It has been shown that there is a distinct advantage in using local origins in these calculations and three ways of doing these are typified by the gauge-including atomic orbitals (GIAO), the independent gauge for local orbitals (IGLO), and the localized orbital-local origin (LORG) approaches. The relative merits and typical successes of these methods have been reviewed.[8] The first, originated by Ditchfield,[9] has been used extensively by Chesnut and coworkers,[10] and more recently, adapted by Pulay.[11] The second was originated by Schindler and Kutzelnigg and used extensively by them[12–14] and also by Grant and coworkers.[15–18] LORG, the method chosen here, was originated by Hansen and Bouman.[19–21] These methods do not include correlation effects. Hansen and Bouman have recently included second-order correlation in shielding calculations and they have found for ^{31}P shielding in PH_3 and also in P_4 molecules only small contributions of second-order correlation, although the latter are quite important for multiply bonded cases such as PN and NNO.[22,23] In this work, we use the LORG method. Ammonia has six normal modes; these vibrations can be expressed in terms of the six symmetry coordinates for NH_3,

$$\begin{aligned}
S_1 &= (1/\sqrt{3})(\Delta r_1 + \Delta r_2 + \Delta r_3),\\
S_2 &= (1/\sqrt{3})r_e(\Delta\alpha_1 + \Delta\alpha_2 + \Delta\alpha_3),\\
S_{3a} &= (1/\sqrt{6})(2\Delta r_1 - \Delta r_2 - \Delta r_3),\\
S_{3b} &= (1/\sqrt{2})(\Delta r_2 - \Delta r_3),\\
S_{4a} &= (1/\sqrt{6})r_e(2\Delta\alpha_1 - \Delta\alpha_2 - \Delta\alpha_3),\\
S_{4b} &= (1/\sqrt{2})r_e(\Delta\alpha_2 - \Delta\alpha_3),
\end{aligned} \quad (3)$$

only two of which are fully symmetric. These are the symmetric stretch and the inversion modes. The first-order contribution would mainly come from these two as a result of symmetry considerations. This paper will account for the other modes as well since they give significant higher-order contributions.

Self-consistent-field (SCF) and shielding calculations were all done on an IBM 3090/300J/VECTOR FACILITY running CMS/SP under VM/XA. GAUSSIAN 88 (Ref. 24) is used to generate the necessary SCF information at different molecular geometries. The calculation of the shielding at each geometry is carried out with RPAC version 8.5 (Ref. 25) by Hansen and Bouman which employs the localized orbital-local origin (LORG) method. The N–H bond length is varied from its equilibrium value of 1.011 (Ref. 26) to 0.4 Å, while fixing the bond angle at equilibrium 106.7°.[27] Nine points lie close to the equilibrium geometry and each one is 0.01 Å from its nearest neighbor to assure a good estimate of the first derivative of the shielding with respect to bond length changes at equilibrium. To have a good picture of the shielding behavior far from equilibrium, eight more points are added, spaced by 0.1 Å. All 17 points are considered in obtaining the first and second derivatives of the shielding with respect to S_1.

For the inversion mode, calculations are performed with a convenient coordinate, the angle the N–H bond makes with the C_3 symmetry axis. Due to symmetry, one needs to look at half of the plane only. Fifteen points within 46° from planarity are taken into account. The outer limit of 46° from the planar configuration is chosen after obtaining numerical solutions to the Schrödinger inversion problem and finding out the turning points of the vibrational wave functions.

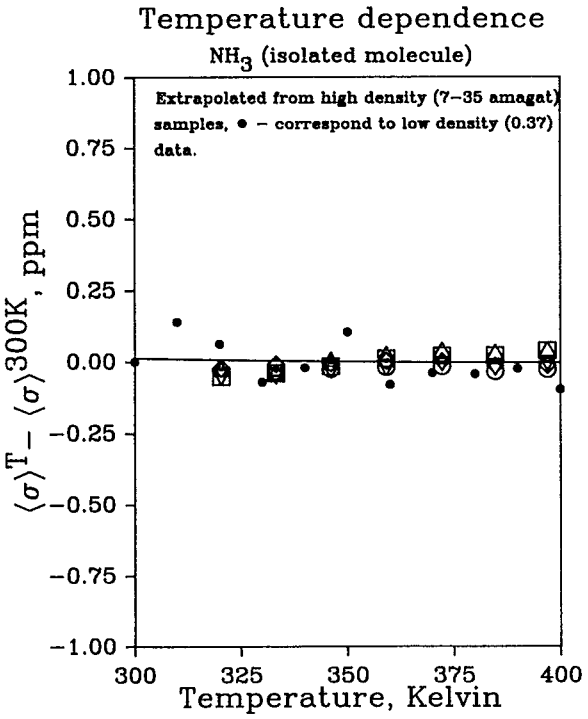

FIG. 3. ^{15}N shielding in NH_3 in the limit of zero density.

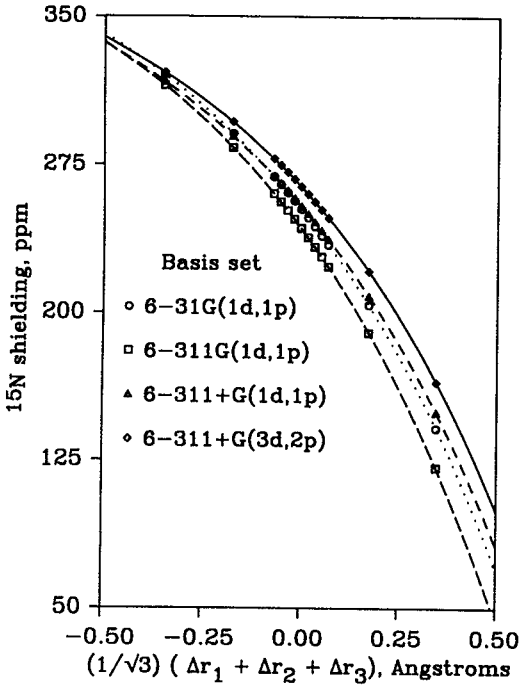

FIG. 4. The shielding as a function of the symmetry coordinate S_1 derived from various basis sets.

To study the basis set dependence of the shielding surfaces, four basis sets are used 6-31G(1*d*,1*p*), 6-311G(1*d*,1*p*), 6-311 + G(1*d*,1*p*) and 6-311 + G(3*d*,2*p*). These are all standard basis sets from Pople.[28] Basis sets smaller than these are clearly inadequate for calculation of nitrogen shielding in ammonia.[29] Although the basis sets employed here provide somewhat different isotropic shielding values, the shielding surfaces from the different basis sets are qualitatively in good agreement, as shown in Figs. 4 and 5. In the finer details, the inversion contribution seems to be sensitive to the choice of basis sets, while the symmetric stretch contribution is less so.

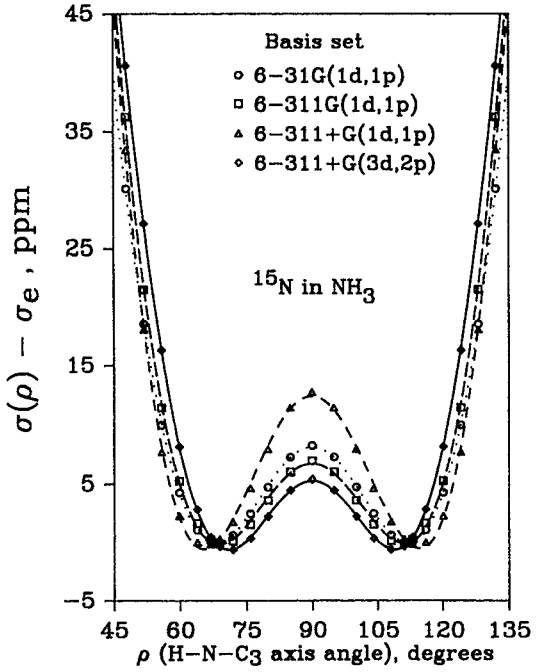

FIG. 5. The shielding as a function of the inversion coordinate derived from various basis sets.

All basis sets show the same behavior of the shielding anisotropy over the different values of the two symmetric coordinates. All seem to show that the inversion corrections are dominated by the perpendicular components. There are minor differences, however. The parallel contribution given by the smallest basis set is relatively small; using a larger basis set with or without diffuse functions makes the parallel contribution go in a direction opposite to that of the perpendicular contribution. Adding diffuse functions increases the perpendicular contribution. In all four basis sets, the shielding anisotropy increases in magnitude as the molecule approaches planarity as expected from physical intuition.

It is especially important to have the flexibility in the basis set to describe $\sigma(S_2)$ in the planar configuration as well as the pyramidal configuration. It is noteworthy to mention that Trudeau and Farrar have observed that including diffuse functions tends to improve the shielding calculations for central atoms.[29,30] The choice is made based on how close the results are to the experimental (spin-rotation-derived) isotropic shielding value and anisotropy.[31(a)] The 6-311 + G(3*d*,2*p*) basis set seems to perform best in reproducing both the isotropic shielding value and the anisotropy at equilibrium geometry (see Table I). The SCF energy obtained using 6-311 + G(3*d*,2*p*) is also satisfactory in predicting the inversion barrier height 2190 cm^{-1}. This result compares favorably with the relatively larger basis set calculations of Spirko: 1980 cm^{-1} using [8*s*5*p*3*d*/6*s*2*p*].[31(b)] From Table I, it is clear that multiple sets of polarization functions on nitrogen and hydrogen are necessary. Adding diffuse functions on hydrogen does not alter the results of the calculations. To save time and effort, calculations for the shielding dependence on the asymmetric modes are done only with the 6-311 + G(3*d*,2*p*) basis set.

Calculations are carried out on 13 additional geometries involving a change only in the S_3 coordinate. For S_4, 12 more points are obtained. To evaluate the cross terms, nine

TABLE I. Basis set dependence of the nitrogen shielding in NH_3 at the equilibrium geometry.

Basis set	σ_e (ppm)	$(\sigma_\parallel - \sigma_\perp)$ (ppm)
6-31G(1*d*, 1*p*)	252.61	− 14.37
6-311G(1*d*, 1*p*)	242.96	− 25.54
6-311 + G(1*d*, 1*p*)	254.18	− 38.59
6-311G(2*d*, 1*p*)	246.90	− 23.28
6-311G(2*d*, 2*p*)	252.41	− 24.27
6-311 + G(2*d*, 1*p*)	256.91	− 36.78
6-311G(3*d*, 2*p*)	252.86	− 25.74
6-311 + G(3*d*, 2*p*)	263.99	− 38.00
Expt.[a]	264.5 ± 0.05	− 40

[a] Reference 31. This experimental value is derived from the measured components of the spin-rotation tensor for the NH_3 molecule in its ground vibrational state and does not include vibrational corrections.

more points, where S_1 and S_2 coordinates are varied simultaneously, are used to determine the shielding mixed second derivative with respect to S_1 and S_2 and an additional nine points to extract the shielding mixed second derivative with respect to S_3 and S_4. All these add up to a total of 75 geometries. Figure 6 shows the dependence of the shielding on each of the symmetry coordinates other than inversion. Only the traces on the shielding surface with respect to variation of S_{3b} and S_{4b} are shown. S_{3a} and S_{4a} have the same traces.

Not surprisingly, the variation of N shielding with the symmetric N–H stretch is typical, i.e., a negative first derivative of shielding with respect to bond stretching, the same as had been deduced empirically from isotope shift data to be a global characteristic.[32] Recent calculations show this typical sign[10,33–40] and also show that the second derivatives with respect to bond stretch are commonly negative,[37–39,41] as we have found here for NH_3. The vanishing first derivatives with respect to asymmetric coordinates are dictated by symmetry. The signs of the second derivatives with respect to asymmetric coordinates are the same as in CH_4, negative (and large) for asymmetric stretch and positive (and small) for asymmetric bond angle change.[38]

Some conclusions can be drawn from the general features of these surfaces even before rovibrational averaging is carried out. The first derivative of the shielding with respect to increasing bond length $(\partial\sigma/\partial r)_e$ is negative in all three basis sets. From bond stretching alone, a negative temperature coefficient $[(\partial\sigma_0/\partial T)<0]$ is therefore expected. For the deuterium-induced isotope shift, considering only the first-order contribution of bond stretching is already satisfactory. All four basis sets yield shielding functions of the inversion coordinate that have their minima nearly coinciding with the minima of the inversion potential. Consequently, considering only the inversion coordinate, the expectation value for the shielding at some geometry other than equilibrium would be larger than the value at equilibrium. From the very nature of the inversion potential surface, the contribution to the temperature dependence due to inversion has to be positive, opposite to that from bond stretching. Involving heavier isotopes leads to a lower positioning of the inversion levels and gives an isotope shift of sign opposite to that from bond stretching. For ammonia, the final answer will require not only a knowledge of the shape of the shielding surfaces, but also a good estimate of the magnitude of its dependence on these two motions. In addition, second-order contributions cannot be ignored. Due to the huge second derivative of the shielding function with respect to S_1 and S_3 coordinates, the so-called "harmonic corrections" would be

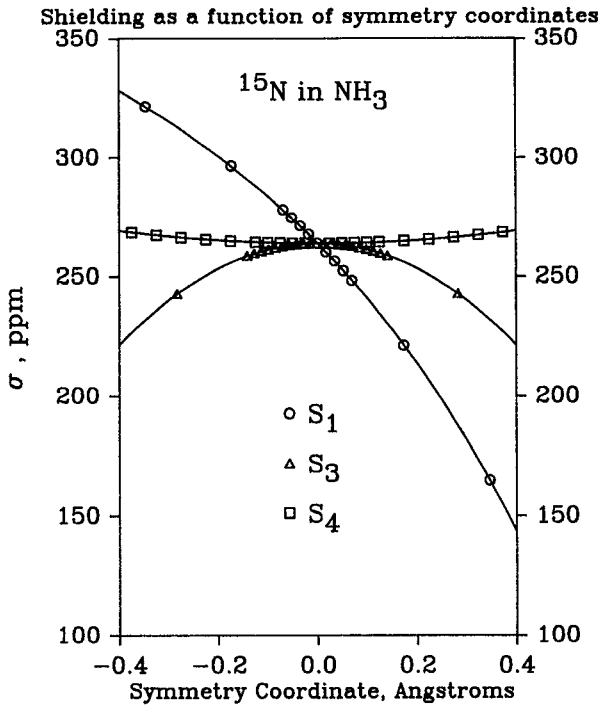

FIG. 6. The shielding as a function of the symmetry coordinates (aside from inversion).

significant enough to affect the results of the calculations. The shielding property behaves in an opposite way with respect to the doubly degenerate S_4 coordinate, although much shallower than the S_3 case (see Fig. 6). The mean-square amplitude of S_4 is bigger, enabling its contribution to somewhat cancel the second-order contributions from the S_1 and S_3 coordinates. Not surprisingly, in earlier work on various other molecules, there has been a great deal of success in simply fitting one parameter, normally the first derivative of the shielding with respect to bond length displacement, to explain observed isotope shifts and temperature dependence of the shielding property.

ROVIBRATIONAL AVERAGING

The traces on the nitrogen shielding surface shown in Fig. 6 which we have calculated here will now be used in obtaining the thermally averaged shielding in NH_3 and ND_3. We express the nitrogen shielding (or any other property P which has the same site symmetry) in ammonia as a series in terms of the symmetry coordinates defined in Eq. (3),

$$P = P_e + P_1 S_1 + (1/2)P_{11}(S_{11})^2 + P_{12}S_1S_2 + (1/2)P_{33}[(S_{3a})^2 + (S_{3b})^2] + (1/2)P_{44}[(S_{4a})^2 + (S_{4b})^2]$$
$$+ P_{34}(S_{3a4a} + S_{3b4b}) + \text{inversion contribution} + P_{122}S_1(S_2)^2 + P_{112}(S_1)^2(S_2)$$
$$+ P_{111}(S_1)^3 + \cdots, \qquad (4)$$
$$\text{inversion contribution} = P_2S_2 + (1/2)P_{22}(S_{22})^2 + (1/6)P_{222}(S_2)^3 + (1/24)P_{2222}(S_2)^4 + \cdots .$$

In this expansion, we have separated out the S_2 coordinate. Since the amplitudes of S_2 are not restricted to small values as the S_1, $S_{3a,b}$, and $S_{4a,b}$ amplitudes are, the inversion coordinate will be treated separately. The derivatives of the property with respect to the symmetry coordinates are $P_1, P_2, P_{11}, P_{12}, P_{22}, P_{33}$, etc.

The shielding can also be expressed in terms of the internal coordinates

$$P = P_e + P_r(\Delta r_i;3) + P_\alpha r_e(\Delta\alpha_i;3) + (1/2)P_{rr}((\Delta r_i)^2;3) + P_{rs}(\Delta r_i\Delta r_j;3) + P_{r\alpha} r_e(\Delta r_i\Delta\alpha_i;3)$$
$$+ P_{r\beta} r_e(\Delta r_i\Delta\alpha_j;6) + (1/2)P_{\alpha\alpha} r_e^2((\Delta\alpha_i)^2;3) + P_{\alpha\beta} r_e^2(\Delta\alpha_i\Delta\alpha_j;3) + \text{higher order terms.} \quad (5)$$

In Eq. (5), we use the shorthand notation adopted by Raynes,[38] i.e., $(\Delta r_i;3)$ stands for the sum of three terms $(\Delta r_1 + \Delta r_2 + \Delta r_3)$, etc.

Equating coefficients from Eqs. (4) and (5), the following relationships are obtained:

$$P_r = P_1/\sqrt{3}, \quad P_{rr} = P_{11}/3 + 2P_{33}/3, \quad P_{rs} = P_{11}/3 - 2P_{33}/3, \quad P_{r\alpha} = P_{12}/3 + 2P_{34}/3, \quad P_{r\beta} = P_{12}/3 - P_{34}/3,$$
$$P_{\alpha\alpha} = P_{22}/3 + 2P_{44}/3, \quad P_{\alpha\beta} = P_{22}/3 - 2P_{44}/3. \quad (6)$$

Higher derivatives can also be related: ($P_{r\alpha\alpha}$, $P_{r\beta\beta}$, $P_{r\alpha\beta}$) in terms of P_{122} ($P_{rr\alpha}$, $P_{rs\alpha}$, $P_{rr\beta}$, $P_{rs\beta}$) in terms of P_{112} etc. The values of the derivatives which were obtained from the surfaces calculated using the 6-311 + G(3*d*,2*p*) basis set are given in Table II. P_{34} is found to be essentially zero in this basis set.

We now consider the inversion mode. Several papers have been published concerning the inversion mode of ammonia.[42-46] The empirical potential function introduced by Spirko, Stone, and Papousek[46] has been chosen here since it remarkably fits the high resolution IR data for ammonia and all its isotopomers.

Since the inversion is treated separately, we can use a more convenient coordinate than S_2. We use the angle between the N–H bond and the threefold symmetry axis (call it ρ). The potential function is in the following parametrized form:

$$V(\rho) = 0.5k(\rho - \pi/2)^2 + a\{\exp[-b(\rho - \pi/2)^2]/[1 + h^2(\rho - \pi/2)^2]\} + c(\rho - \pi/2)^4, \quad (7)$$

which is shown in Fig. 7(a). The parameters *a*, *b*, *c*, *k*, and *h* are given by Spirko *et al.*[46] The equation

$$(h/2\pi)^2[\partial^2\Psi(\rho)/\partial\rho^2] = 6m_H(r_e)^2[\cos^2(\rho_e) + (m_N/M)\sin^2(\rho_e)][V(\rho) - E]\Psi(\rho) \quad (8)$$

is solved by employing the Numerov–Cooley algorithm[47,48] using 1000 points equally spaced between 0 and $\pi/2$. The lowest energy eigenfunctions are shown in Fig. 7(b). The 6-311 + G(3*d*,2*p*) shielding surface shown in Fig. 5 is fitted to a tenth-order polynomial function centered at the planar configuration, which, in turn, is used to create 1000 points for computing the integrals $\langle i|\sigma(S_2) - \sigma_e|i\rangle$ by Simpson's method. These integrals shown in Table III are the vibrationally averaged shielding for each of the inversion levels. The thermal average inversion contribution is calculated by a Boltzmann average

$$\langle\Delta P_{\text{inversion}}\rangle^T = \sum_{i=0^s,\ 0^a,\ 1^s,\ 1^a,\ 2^s,\ 2^a} \exp(-E_i/kT)\langle i|P(\rho)|i\rangle - P_e. \quad (9)$$

The results are shown in Fig. 8. Using the derivatives of the shielding with respect to internal coordinates, one can derive the rovibrationally averaged value for the shielding at any temperature using the following equation:

$$\langle P\rangle^T = P_e + P_r(\Delta r_i;3)^T + (1/2)P_{rr}((\Delta r_i)^2;3)^T + P_{rs}(\Delta r_i\Delta r_j;3)^T + P_{r\alpha} r_e(\Delta r_i\Delta\alpha_i;3)^T$$
$$+ P_{r\beta} r_e(\Delta r_i\Delta\alpha_j;6)^T + (1/3)P_{44} r_e^2((\Delta\alpha_i)^2;3)^T + \text{inversion contribution.} \quad (10)$$

TABLE II. Derivatives of the shielding surface.

P_1	-213.40 ppm/Å
P_2	-12.37 ppm/Å rad
P_{11}	-337.46 ppm/Å^2
P_{22}	112.69 ppm/Å^2 rad^2
P_{33}	-535.94 ppm/Å^2
P_{44}	62.32 ppm/Å^2 rad^2
P_{12}	-19.42 ppm/Å rad
P_{111}	-633.72 ppm/Å^3
P_{112}	-131.03 ppm/Å^3 rad
P_{122}	165.54 ppm/Å^3 rad^2
P_{222}	121.14 ppm/Å^3 rad^3
P_r	-123.21 ppm/Å
P_α	-7.14 ppm/Å rad
P_{rr}	-469.78 ppm/Å^2
P_{rs}	244.81 ppm/Å^2
$P_{r\alpha}$	-6.47 ppm/Å^2 rad
$P_{r\beta}$	-6.47 ppm/Å^2 rad
$P_{\alpha\alpha}$	79.11 ppm/Å^2 rad^2
$P_{\alpha\beta}$	-3.98 ppm/Å^2 rad^2

All that is needed now is to evaluate the thermal average values of the various internal coordinates at a specified temperature. The treatment used in this paper is identical to the one employed by Jameson and Osten.[4] Bartell's method[49] is used in the determination of the anharmonic contribution to bond length stretching, making the usual approximation for the mean-square amplitude, i.e., $\langle Q_i^2\rangle = (h/8\pi^2 c\omega_i)\coth(hc\omega_i/2kT)$, and using the force constants presented in Ref. 46. Toyama, Oka, and Morino have provided the equation that gives the centrifugal distortion contribution to bond length stretching and bond angle deformation.[50] The shielding corrections from these modes other than inversion are given in Table IV.

Although we have calculated the inversion contribution fairly completely, we have only included up to quadratic terms in the other symmetry coordinates in calculating the thermal average shielding. We have left out contributions to the shielding from S_1^3, $S_1^2S_2$, $S_1S_2^2$, $S_1S_3^2$, $S_2S_3^2$, $S_1S_4^2$, $S_2S_4^2$, $S_1S_3S_4$, $S_2S_3S_4$, and higher-order terms. Since the inversion motion involves relatively large displacements from equilib-

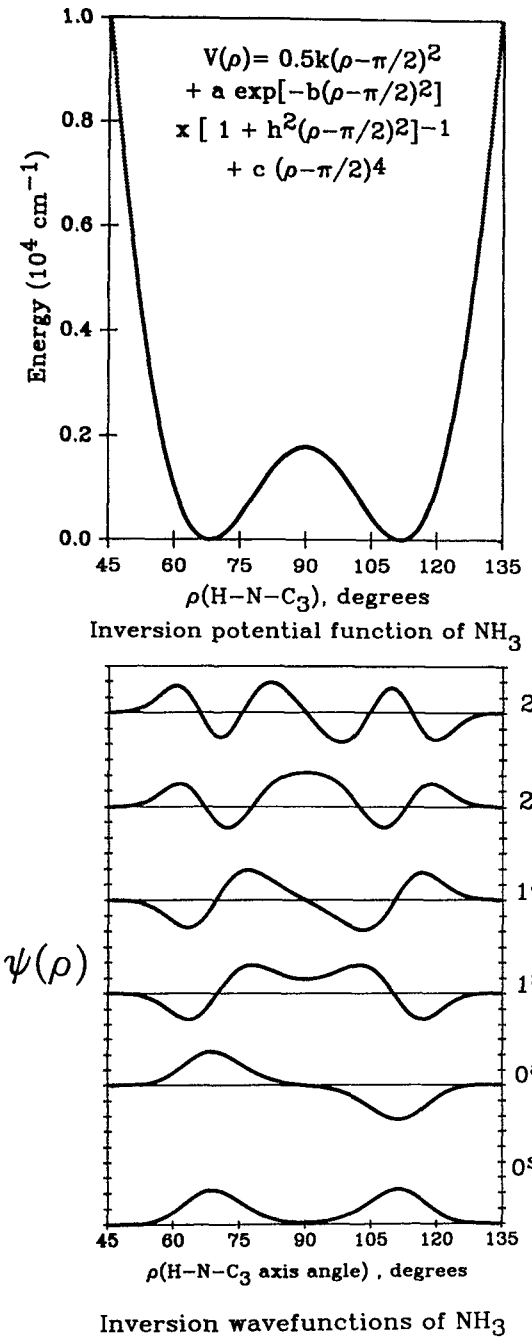

FIG. 7. (a) The empirical potential function for the inversion of ammonia (Ref. 46). (b) Numerical solutions to the inversion problem.

TABLE III. Inversion corrections to shielding for various states.

	$\langle i\|\sigma(S_2)-\sigma_e\|i\rangle$ (ppm)	
i	NH_3	ND_3
0^s	0.914	0.629
0^a	0.907	0.628
1^s	3.020	2.161
1^a	2.837	2.126
2^s	4.500	3.829
2^a	4.465	3.489

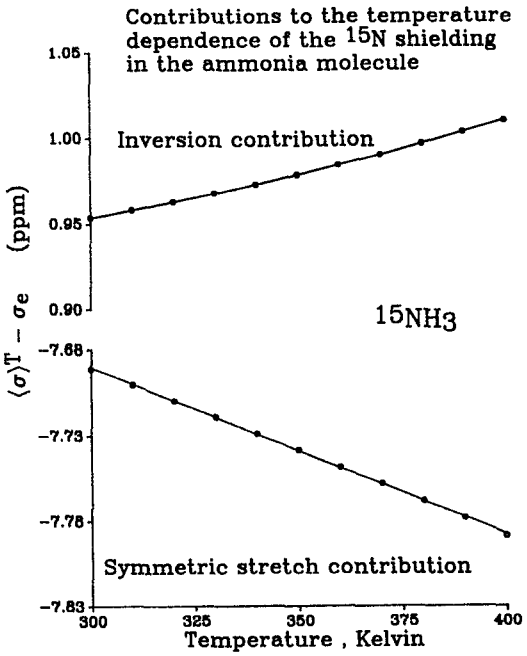

FIG. 8. Two major contributions to the temperature dependence of the ^{15}N shielding in $^{15}NH_3$ are shown here: all terms in the inversion coordinate and the leading term in the symmetric stretch. Detailed contributions are given in Tables IV–VI.

rium, the terms involving S_2 may not be insignificant enough to be neglected. Terms not involving S_2 would be small since these only concern small amplitude motions. P_{111} is also large enough to be considered, even though it does not involve any inversion term. Hence, we examine how large these contributions are. The third shielding derivatives are shown below

$$P_{111} = -633.72 \text{ ppm/Å}^3,$$
$$P_{112} = -131.03 \text{ ppm/Å}^3 \text{ rad},$$
$$P_{122} = +165.54 \text{ ppm/Å}^3 \text{ rad}^2.$$

These were obtained from the same geometries that gave the first and second derivatives of the shielding with respect to the various symmetry coordinates. The thermal averages for the following terms: $\langle S_1^2 S_2\rangle^T$, $\langle S_1^3\rangle^T$, and $\langle S_1 S_2^2\rangle^T$ have been approximated by $\langle S_1^2\rangle^T\langle S_2\rangle^T$, $\langle S_1^2\rangle^T\langle S_1\rangle^T$, and $\langle S_1\rangle^T\langle S_2^2\rangle^T$, respectively.

These terms turn out to be very small and they come in oppositely signed pairs and nearly cancel each other out. Together these provide the additional rovibrational corrections collectively referred to as higher-order contributions in Table V. These are about three orders of magnitude smaller than the rovibrational terms contributing to shielding in NH_3 and ND_3 which have been calculated at the quadratic level.

The total nitrogen shielding in NH_3 and ND_3 as a function of temperature is shown in Table V and Fig. 9. The negative temperature dependence is clearly coming from the rotational (centrifugal stretching) contribution. The stretching vibrational levels are so high in energy that contributions to the property average from the higher vibrational

TABLE IV. Shielding corrections (ppm) at various temperatures considering coordinates other than inversion.

	Temperature (K)	P_r	P_{rr}	P_{rs} (10^{-3})	$P_{r\alpha}$ (10^{-3})	$P_{r\beta}$ (10^{-3})	P_{44}
NH_3	300	−7.691	−3.585	5.08	3.35	18.82	1.536
	310	−7.700	−3.585	5.24	3.39	18.86	1.537
	320	−7.710	−3.585	5.42	3.44	18.90	1.539
	330	−7.719	−3.586	5.61	3.48	18.95	1.540
	340	−7.729	−3.586	5.82	3.53	19.00	1.542
	350	−7.739	−3.586	6.04	3.58	19.06	1.544
	360	−7.748	−3.586	6.28	3.64	19.12	1.547
	370	−7.758	−3.586	6.53	3.70	19.19	1.549
	380	−7.768	−3.587	6.80	3.77	19.26	1.552
	390	−7.778	−3.587	7.08	3.83	19.33	1.554
	400	−7.789	−3.587	7.38	3.90	19.40	1.557
ND_3	300	−5.643	−2.620	−13.07	1.208	17.06	1.148
	310	−5.653	−2.620	−12.78	1.279	17.14	1.151
	320	−5.663	−2.621	−12.48	1.356	17.22	1.155
	330	−5.674	−2.621	−12.15	1.436	17.30	1.159
	340	−5.684	−2.621	−11.81	1.520	17.38	1.163
	350	−5.695	−2.622	−11.45	1.607	17.48	1.167
	360	−5.706	−2.622	−11.08	1.699	17.58	1.171
	370	−5.717	−2.622	−10.69	1.793	17.68	1.176
	380	−5.728	−2.623	−10.28	1.891	17.78	1.181
	390	−5.739	−2.623	−9.86	1.992	17.89	1.186
	400	−5.751	−2.624	−9.43	2.096	18.01	1.192

states do not significantly change with temperature in the temperature range that we are considering. The derivatives of the shielding with respect to bond stretching are significantly larger compared to the derivatives with respect to bond angle deformations. This leads to the rovibrational corrections ($\langle\sigma\rangle^T - \sigma_e$) being dominated by bond stretching contributions. However, the temperature dependence relies on how accessible the higher vibrational states are. Bending motions are normally of lower frequencies and, thus, more accessible and can contribute to the temperature dependence of the shielding. In the case of ammonia, the shielding dependence on the inversion and S_4 coordinates leads to positive contributions to the temperature dependence. There is a possibility that these could outweigh the negative contribution to the temperature dependence from centrifugal stretching.

Results of our calculations show that the lighter isoto-

TABLE V. Shielding corrections (ppm) at various temperatures (all coordinates).

	Temperature (K)	Inversion	Other modes	Higher-order contributions	Total
NH_3	300	0.9537	−9.7133	−0.0458	−8.8054
	310	0.9580	−9.7210	−0.0458	−8.8088
	320	0.9626	−9.7287	−0.0458	−8.8119
	330	0.9675	−9.7363	−0.0458	−8.8146
	340	0.9727	−9.7439	−0.0458	−8.8169
	350	0.9782	−9.7514	−0.0458	−8.8189
	360	0.9841	−9.7588	−0.0458	−8.8205
	370	0.9902	−9.7661	−0.0457	−8.8217
	380	0.9966	−9.7734	−0.0457	−8.8225
	390	1.0033	−9.7806	−0.0457	−8.8230
	400	1.0102	−9.7878	−0.0457	−8.8232
ND_3	300	0.6854	−7.1097	−0.0254	−6.4496
	310	0.6916	−7.1163	−0.0254	−6.4501
	320	0.6980	−7.1228	−0.0254	−6.4501
	330	0.7048	−7.1292	−0.0254	−6.4498
	340	0.7119	−7.1355	−0.0254	−6.4490
	350	0.7193	−7.1417	−0.0254	−6.4479
	360	0.7269	−7.1479	−0.0254	−6.4465
	370	0.7348	−7.1540	−0.0254	−6.4447
	380	0.7429	−7.1601	−0.0254	−6.4426
	390	0.7513	−7.1661	−0.0254	−6.4403
	400	0.7598	−7.1721	−0.0254	−6.4377

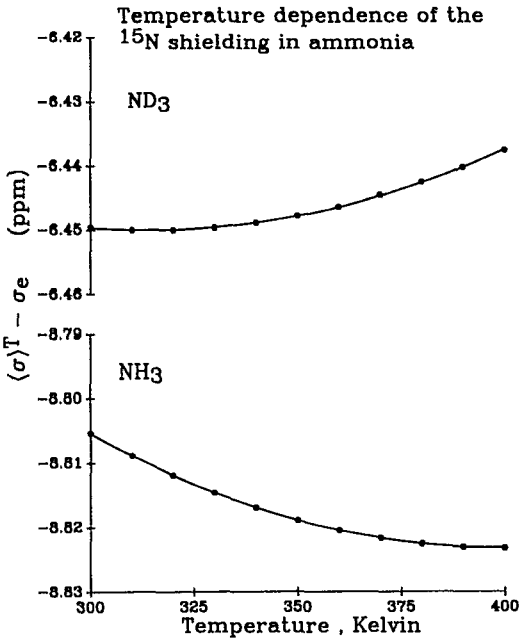

FIG. 9. *Ab initio* results for the temperature dependence of the ^{15}N shielding in NH_3 and ND_3.

pomer seems to be reaching a minimum at ~400 K. Within the temperature range of this study (300–400 K), contributions from centrifugal distortion are dominant and the shielding decreases with increasing temperature. However, near 400 K, contributions from the inversion and asymmetric bending motions start to offset the negative temperature dependence and may even outweigh bond stretching contributions at higher temperatures. For the heavier isotopomer, the resulting temperature dependence is already positive almost throughout the range of 300–400 K. The minimum for the heavier isotopomer occurs at 320 K. The calculated temperature dependence for the two isotopomers of ammonia is shown in Fig. 9. The difference between the two isotopomers is as expected from the vibrational levels being closer in energy to each other in ND_3 than in NH_3. Our results look similar to those obtained by Raynes and co-workers on the temperature dependence of the ^{13}C shielding in various methane isotopomers.[7]

DISCUSSION

The relatively flat temperature dependence of the shielding has the following consequences on both theory and experiment: Since there are opposing contributions of comparable magnitude, the results are sensitive to errors in computations. We have calculated a reasonably well-defined temperature dependence of the nitrogen shielding for the inversion coordinate, likewise for the dependence on temperature due to all other coordinates. However, because they nearly offset each other, the overall result shown in Fig. 9 is not so well defined. With regard to experiment, it will not be so surprising to face great difficulty in obtaining excellent results. Intermolecular effects in gas-phase NMR experiments generally tend to decrease shielding.[51] These effects are also known to increase in magnitude as the temperature is lowered.[52] Samples at higher densities then exhibit a positive temperature dependence of the shielding if the isolated molecule's intrinsic temperature dependence is flat. With the high density samples (7–33 amagat), extrapolation to the zero density limit leaves a residual very slight positive temperature dependence for the ^{15}N shielding in NH_3. The samples at very low densities, where intermolecular effects are small (0.37–1.5 amagat) can provide limiting values for the intrinsic temperature dependence of N shielding. The experimental temperature dependence of nitrogen shielding in ammonia is so small that extremely fortunate conditions are required to see it. In our experiments, the stability of the magnet has been ascertained to 0.01 ppm over a period of 24 h and over a range of 100° (300–400 K). (At a magnetic field of 9.4 tesla, 0.01 ppm translates to 0.4 Hz in the ^{15}N resonance frequency.) At low densities, the natural ^{15}N relaxation times are such that the peaks have significantly broadened, making it difficult to locate the center of the peak precisely. With Lorentzian fitting, the uncertainty of finding the center is reduced to 3 Hz. In Fig. 3, the scatter in the 0.37 amagat sample reflects this uncertainty.

How good is our experimental $\sigma_0(T)$? As we can see in Fig. 3, we have considerable scatter at the low densities because of greater linewidths at these densities. On the other hand, the $\sigma_0(T)$ obtained from the 7–33 amagat samples after subtracting out $\sigma_1(T)\rho$ have somewhat less scatter, even though these include five samples with attendant density errors. Due to the limitation in the temperature range for the higher density samples, these points only span 335–400 K. The 0.37 amagat sample has a nearly flat temperature dependence, or if it can be believed, a normal one. The experimental data in Fig. 3 are consistent with the calculated temperature dependence in Fig. 9. The calculated total change for NH_3 in the range 300–400 K is -0.01 ppm, certainly within the experimental errors in Fig. 3. Since the two parts, the inversion, and the rest have opposite and nearly canceling temperature dependencies, the net slight temperature dependence shown in Fig. 9 can have considerable systematic error. The agreement between the solid curve shown in Fig. 3 (the theoretical curve from Fig. 9) and the individual experimental points is as good as can be expected.

Our other comparison with experiment is the isotope shift. Here the only value available is in the neat liquid phase at 293 K $[\sigma_0(ND_3) - \sigma_0(NH_3)] = 1.87$ ppm.[5] We calculate 2.36 ppm.

How important are the various calculated terms in the rovibrational corrections to the temperature dependence and to the isotope shift? We show these in Table VI. The P_r term gives the largest contribution to the rovibrational correction (-7.7 ppm for NH_3 at 300 K) with P_{rr}, P_{44}, and the inversion the next largest. Altogether, due to canceling opposite-signed terms, the latter three constitute a rovibrational correction of -1 ppm at 300 K. The calculated temperature dependence in NH_3 is very small due to the inversion and S_4 having a positive temperature dependence, whereas all others exhibit a negative temperature dependence. The net result for ^{15}N in NH_3, if it can be believed, exhibits the usual behavior, as the P_r stretch contribution

TABLE VI. Contributions (in ppm) of various terms in nitrogen shielding.

Term	Vibrational correction at 300 K $\sigma(300\ \mathrm{K}) - \sigma_e$		Temperature dependence $\sigma(400\ \mathrm{K}) - \sigma(300\ \mathrm{K})$		Isotope shift $\sigma(\mathrm{ND_3}) - \sigma(\mathrm{NH_3})$	
	NH_3	ND_3	NH_3	ND_3	300 K	400 K
P_r	−7.69	−5.64	−0.097	−0.108	2.05	2.04
P_{rr}	−3.59	−2.62	−0.002	−0.004	0.97	0.96
$P_{r\alpha}$	0.01	−0.01	0.002	0.004	−0.02	−0.02
$P_{r\alpha} + P_{r\beta}$	0.02	0.02	0.001	0.002	−0.004	−0.003
P_{44}	1.54	1.15	0.021	0.044	−0.39	−0.37
Sum[a]	−9.71	−7.10	−0.075	−0.062	2.61	2.61
Inversion	0.95	0.69	0.057	0.074	−0.27	−0.25
Higher order[b]	−0.05	−0.03	0.0001	−0.0001	0.02	0.02
Total	−8.81	−6.45	−0.018	0.012	2.36	2.39

[a] Sum of the above five terms.
[b] Terms in $P_{111}S_1^3 + P_{122}S_1S_2^2 + P_{112}S_1^2S_2$.

(usual sign) including the rotational part, wins out slightly over all other terms. On the other hand, the isotope shift is largely determined by the P_r contribution, with the inversion contribution being opposite in sign, but only about 10% of the total. It is not surprising, therefore, that previous empirical estimates of P_r derived from isotope shifts agree quite well with *ab initio* values.

Further progress in the calculations will require second-order electron correlation calculations. The calculated values of the shielding tensor components at the equilibrium geometry are very close to the values derived from spin rotation constants. These, however, do not include the rovibrational corrections. The latter would make the discrepancy between theoretical and experimental values larger than shown in Table I, suggesting an overestimation of the paramagnetic part of the shielding. On the other hand, in a recent study made by Hansen and Bouman on a similar molecule PH_3,[22] the inclusion of second-order electron correlation in the calculation of the ^{31}P shielding in PH_3 shows these to be relatively unimportant.

It is also necessary to point out that the rovibrational corrections presented in this paper are dependent on the choice of equilibrium geometry because of the nonzero second derivatives of the shielding surfaces. Since the second derivative for the modes involving bond length displacements are negative, the use of bond lengths obtained by optimization of geometry (which are found to be shorter than the experimental value) would result in a lowering of the first-order corrections from the symmetric stretch contribution. The problem with this approach suggested by Chesnut[41] is that, if one adopts it, there is no clear choice of the level of computation and the basis set which should be used for geometry optimization. In our work, the rovibrational corrections are given with respect to the isotropic shielding value calculated at the experimental equilibrium geometry. Finally, we compare our results at the equilibrium geometry with previous *ab initio* calculations by other workers in Table VII. Calculations of P_r and P_{rr} by Chesnut and Wright[53] agree reasonably well with our results: $P_r = -126.4$ ppm Å^{-1} (compared to our value -123.21) and $P_{rr} = -470.2$ ppm Å^{-2} (compared to our value -469.78).

CONCLUSIONS

In both NH_3 and ND_3, the contribution of inversion to the total rovibrational corrections to the N shielding is $\sim 15\%$ of the other contributions and opposite in sign. The contributions of inversion to the temperature dependence of

TABLE VII. Comparison of results from various *ab initio* calculations of nitrogen shielding in ammonia.

Method	Basis set	σ_e (ppm)	$\sigma_\parallel - \sigma_\perp$ (ppm)	Reference
This work	6-311 + G(3*d*,2*p*)	263.99	−38.00	
GIAO-MP2 (optimized geometry)	6-31G(1*d*,1*p*)	281.1		54
Conventional CHF	[8*s*6*p*4*d*/6*s*3*p*]	262.09	−39.01	55
IGLO	[7*s*5*p*4*d*/4*s*2*p*]	265.4	−37.7	12
GIAO (optimized geometry)	[4*s*3*p*1*d*/2*s*]	265.2	−45.2	34
CHF	[10*s*6*p*3*d*/5*s*2*p*]	266.13	−40.4	56

the N shielding in ammonia and to the deuterium-induced N shielding change are opposite in sign to the contributions of the other rovibrationally averaged coordinates. The inversion contribution to the isotope shift is small compared to the others so that the sign and magnitude of the isotope shift is normal. On the other hand, the contribution of inversion to the temperature dependence is nearly equal to that due to all others, so the net temperature dependence is very small. Experimental measurements are consistent with these theoretical results.

ACKNOWLEDGMENT

This work has been supported by the National Science Foundation (Grant CHE-8901426).

[1] C. J. Jameson, A. K. Jameson, S. M. Cohen, H. Parker, D. Oppusunggu, P. M. Burrell, and S. Wille, J. Chem. Phys. **74**, 1608 (1981).
[2] C. J. Jameson, A. K. Jameson, and H. Parker, J. Chem. Phys. **68**, 2868 (1978).
[3] C. J. Jameson, A. K. Jameson, and A. C. de Dios (ongoing work).
[4] C. J. Jameson and H. J. Osten, J. Chem. Phys. **82**, 4595 (1985).
[5] R. E. Wasylishen and J. O. Friedrich, Can. J. Chem. **65**, 2238 (1987).
[6] C. J. Jameson, A. K. Jameson, and J. W. Moyer, J. Chem. Phys. **68**, 2873 (1978).
[7] W. T. Raynes, P. W. Fowler, P. Lazzeretti, R. Zanasi, and M. Grayson, Mol. Phys. **64**, 143 (1988).
[8] C. J. Jameson, Nucl. Magn. Reson. **16**, 1 (1987); **18**, 1 (1989); **19**, 1 (1990).
[9] R. Ditchfield, Mol. Phys. **27**, 789 (1974).
[10] D. B. Chesnut and C. K. Foley, J. Chem. Phys. **84**, 852 (1986).
[11] K. Wolinski, J. Hinton, and P. Pulay, J. Am. Chem. Soc. **112**, 8251 (1990).
[12] M. Schindler and W. Kutzelnigg, J. Chem. Phys. **76**, 1919 (1982).
[13] M. Schindler and W. Kutzelnigg, J. Am. Chem. Soc. **105**, 1360 (1983).
[14] M. Schindler, J. Am. Chem. Soc. **109**, 5950 (1987).
[15] A. J. Beeler, A. M. Orendt, D. M. Grant, P. W. Cutts, J. Michl, K. W. Zilm, J. W. Downing, J. C. Facelli, M. Schindler, and W. Kutzelnigg, J. Am. Chem. Soc. **106**, 7672 (1984).
[16] J. C. Facelli, A. M. Orendt, A. J. Beeler, M. S. Solum, G. Depke, K. D. Malsch, J. W. Downing, P. S. Murthy, D. M. Grant, and J. Michl, J. Am. Chem. Soc. **107**, 6749 (1985).
[17] C. M. Carter, D. W. Alderman, J. C. Facelli, and D. M. Grant, J. Am. Chem. Soc. **109**, 2639 (1987).
[18] J. C. Facelli, D. M. Grant, and J. Michl, Int. J. Quantum Chem. **31**, 45 (1987).
[19] A. E. Hansen and T. D. Bouman, J. Chem. Phys. **82**, 5035 (1985).
[20] A. E. Hansen and T. D. Bouman, J. Chem. Phys. **91**, 3552 (1989).
[21] T. D. Bouman and A. E. Hansen, Chem. Phys. Lett. **149**, 510 (1988).
[22] T. D. Bouman and A. E. Hansen, Chem. Phys. Lett. **175**, 292 (1990).
[23] T. D. Bouman and A. E. Hansen, presented at the Danish Chemical Society Meeting, Odense June 7, 1990.
[24] M. J. Frisch, M. Head-Gordon, H. B. Schlegel, K. Raghavachari, J. S. Binkley, C. Gonzalez, D. J. Fox, R. A. Whiteside, R. Seeger, C. F. Melius, J. Baker, R. Martin, L. R. Kahn, J. J. P. Stewart, E. M. Fluder, S. Topial, and J. A. Pople, Gaussian, Inc., Pittsburgh, PA, 1988.
[25] RPAC version 8.5, Thomas D. Bouman, Southern Illinois University at Edwardsville, and Aage E. Hansen, H. C. Oersted Institute, Denmark.
[26] Y. Morino, K. Kuchitsu, and S. Yamamoto, Spectrochim. Acta Part A **24**, 335 (1968).
[27] W. S. Benedict and E. K. Plyer, Can. J. Phys. **35**, 1235 (1957).
[28] R. Krishnan, J. S. Binkley, R. Seeger, and J. A. Pople, J. Chem. Phys. **72**, 650 (1980).
[29] J. Trudeau and T. C. Farrar (private communications).
[30] J. Trudeau and T. C. Farrar, J. Phys. Chem. **94**, 6277 (1990).
[31] (a) S. G. Kukolich, J. Am. Chem. Soc. **97**, 5704 (1975); (b) V. Spirko and W. P. Kraemer, J. Mol. Spectrosc. **133**, 331 (1989).
[32] C. J. Jameson, J. Chem. Phys. **66**, 4977 (1977).
[33] D. B. Chesnut, Chem. Phys. **110**, 415 (1986).
[34] D. B. Chesnut and C. K. Foley, J. Chem. Phys. **85**, 2814 (1986).
[35] U. Fleischer, M. Schindler, and W. Kutzelnigg, J. Chem. Phys. **86**, 6337 (1987).
[36] M. Schindler and W. Kutzelnigg, Mol. Phys. **48**, 781 (1983).
[37] R. Ditchfield, Chem. Phys. **63**, 185 (1981).
[38] P. Lazzeretti, R. Zanasi, A. J. Sadlej, and W. T. Raynes, Mol. Phys. **62**, 605 (1987).
[39] P. W. Fowler, G. Riley, and W. T. Raynes, Mol. Phys. **42**, 1463 (1981).
[40] B. Bennett and W. T. Raynes, Spectrochim. Acta Part A **45**, 1267 (1989).
[41] D. B. Chesnut and C. G. Phung, J. Chem. Phys. **91**, 6238 (1989).
[42] A. Rauk, L. C. Allen, and E. Clementi, J. Chem. Phys. **52**, 4133 (1970).
[43] R. M. Stevens, J. Chem. Phys. **61**, 2086 (1974).
[44] J. D. Swalen and J. A. Ibers, J. Chem. Phys. **36**, 1914 (1962).
[45] V. Spirko, J. Mol. Spectrosc. **101**, 30 (1983)
[46] V. Spirko, J. M. R. Stone, and D. Papousek, J. Mol. Spectrosc. **60**, 159 (1976).
[47] B. Numerov, Publ. Observ. Central Astrophys. Pruss. **2**, 138 (1933).
[48] J. W. Cooley, Math. Comp. **15**, 363 (1961).
[49] L. S. Bartell, J. Chem. Phys. **38**, 1827 (1963).
[50] M. Toyama, T. Oka, and Y. Morino, J. Mol. Spectrosc. **13**, 193 (1964)
[51] C. J. Jameson and A. K. Jameson, Mol. Phys. **20**, 957 (1971).
[52] C. J. Jameson, A. K. Jameson, and S. M. Cohen, J. Chem. Phys. **59**, 4540 (1973).
[53] D. B. Chesnut and D. W. Wright (to be published).
[54] E. C. Vauthier, M. Comeau, S. Odiot, and S. Fliszar, Can. J. Chem. **66**, 1781 (1988).
[55] P. Lazzeretti, R. Zanasi, and R. Bursi, J. Chem. Phys. **89**, 987 (1988).
[56] R. Holler and H. Lischka, Mol. Phys. **41**, 1017 (1980).